J Eng Math (2008) 61:399–411
DOI 10.1007/s10665-008-9217-3

The influence of dissipative heating on active vibration damping of viscoelastic plates

V. G. Karnaukhov · I. F. Kirichok · M. V. Karnaukhov

Received: 14 March 2007 / Accepted: 11 February 2008 / Published online: 30 April 2008
© Springer Science+Business Media B.V. 2008

Abstract A mathematical formulation of a new nonlinear problem for active vibration damping (ACD) of thin viscoelastic plates by distributed piezoelectric sensors and actuators is given. The influence of dissipative heating on ACD is considered. The nonlinearity of the problem is caused by the temperature dependence of the material properties and the nonlinearity of the dissipative function. The thermomechanical behavior of the materials under harmonic loading is described by the concept of complex characteristics. Numerical and analytical methods are used for solving this problem. As an example, the influence of dissipative heating on damped axisymmetric bending vibrations of a circular viscoelastic plate is investigated. It is shown that this influence can be significant in the case of ACD of polymeric plates.

Keywords Active damping · Circular plate · Dissipative heating · Harmonic load · Sensor and actuator

1 Introduction

Composite viscoelastic plates are widely used as structural elements in different fields of engineering. Piezoelectric materials have been used extensively as sensors and actuators in engineering applications to damp the vibrations of these plates. Structures that are combined with piezoelectric materials serving as sensors and actuators, have been called smart structures and have attracted considerable attention among engineers. In practical applications, active piezoelectric structures are exposed to temperature changes due to (i) external temperature variations; (ii) coupling electromechanical and thermal fields (pyro-effect); (iii) dissipative heating of viscoelastic materials. The first and second effects are investigated in [1–5]. Information regarding the third effect is limited and, to authors' best knowledge, reliable analytical relationships reflecting this effect are not currently available. General questions regarding modeling coupled mechanical, electrical and thermal fields with effects of dissipative heating taken into account are considered in [6–14].

The nonlinear piezothermoelastic characteristics and temperature effects of piezoelectric laminated shells were derived by Tzou and Bao [15]. Tzou and Zhou [16] investigated the dynamics, electromechanical coupling, and control of thermal buckling of a nonlinear piezoelectric laminated circular plate undergoing large deformations.

V. G. Karnaukhov (✉) · I. F. Kirichok · M. V. Karnaukhov
Timoshenko Institute of Mechanics, National Academy of Science of Ukraine, Nesterov Str., 3, Kiev 03057, Ukraine
e-mail: term@inmech.kiev.ua

A review of the investigations of ACD of thin-walled elements when the material properties do not depend on temperature, are given in [17–20]. A review of the investigations on the influence of dissipative heating on the behavior of thin-walled elements is considered in [21–26].

The analysis presented here is concerned with the temperature effect of dissipative heating on actively damped resonant vibrations of viscoelastic plates. It is shown that the effect can be significant. Therefore, the efficiency of ACD of plates should be interpreted considering this effect.

2 Formulation of the problem of actively damped forced harmonic thermomechanical vibrations of plates by distributed sensors and actuators

Consider a circular plate ($r_0 \le r \le R$; $0 \le \theta \le 2\pi$) in cylindrical coordinates. The plate is composed of a passive inner layer (without piezo-effect) of thickness h_0, the piezoelectric top and bottom layers having thicknesses h_1 and h_2 with opposite thickness polarization. On the outer surfaces of the piezolayers and on the surfaces between the active and passive layers thin electrodes are coated. The plate is subjected to a harmonic pressure $q(r, \theta, t) = p(r, \theta)\exp(\mathrm{i}\omega t)$ with frequency ω close to resonance. The materials of the layers are viscoelastic. The electromechanical behaviour of the passive and piezo-active layers is described by complex characteristics which depend on temperature.

There are two methods for dealing with ACD of plates when (i) only piezoelectric actuators are used; (ii) piezoelectric sensors and actuators are used. In the first method the potential difference is applied to the actuator to compensate of the mechanical load. In the second method the potential difference applied to the actuator is proportional to a current or first time derivative of the sensor's potential difference.

To study the active vibration damping of plates, the mechanical Kirchhoff–Love hypotheses are introduced with similar hypotheses for the electric-field quantities. It is assumed for elements polarized across the thickness that the tangential components of the electric intensity E_r, E_θ and induction D_r, D_θ are much smaller than the normal components E_z, D_z. As a result, the electrostatic equation takes the form:

$$\frac{\partial D_z}{\partial z} = 0. \tag{1}$$

It follows from (1) that the normal component of the induction is constant throughout the thickness of piezoelectric elements:

$$D_z = C(r, \theta). \tag{2}$$

With these hypotheses we obtain simplified constitutive equations for piezo-active top ($k = 1$) and bottom ($k = 2$) layers:

$$\begin{aligned}
\sigma_{rr}^{(k)} &= B_{11}^{(k)}(z)(\varepsilon_r + z\kappa_r) + B_{12}^{(k)}(z)(\varepsilon_\theta + z\kappa_\theta) - \gamma_{31}^{(k)}(z)E_z^{(k)},\\
\sigma_{\theta\theta}^{(k)} &= B_{12}^{(k)}(z)(\varepsilon_r + z\kappa_r) + B_{22}^{(k)}(z)(\varepsilon_\theta + z\kappa_\theta) - \gamma_{31}^{(k)}(z)E_z^{(k)}, \quad \sigma_{r\theta}^{(k)} = B_{66}^{(k)}(z)(\varepsilon_{r\theta} + z\kappa_{r\theta}),
\end{aligned} \tag{3}$$

$$D_z^{(k)} = \gamma_{33}^{(k)}(z)E_z^{(k)} + \gamma_{31}^{(k)}(z)[(\varepsilon_r + \varepsilon_\theta) + z(\kappa_r + \kappa_\theta)], \tag{4}$$

where for the piezo-active materials we have

$$\begin{aligned}
&B_{11}^{(k)}(z) = B_{22}^{(k)}(z) = 1/S_{11}^{(k)}(z)[1 - \nu^{(k)2}(z)], \quad B_{12}^{(k)}(z) = \nu^{(k)}(z)B_{11}^{(k)}(z),\\
&B_{66}^{(k)}(z) = \frac{1}{2}[1 - \nu^{(k)}(z)]B_{11}^{(k)}(z), \quad \gamma_{33}^{(k)}(z) = \varepsilon_{33}^{T(k)}(z)[1 - k_p^{(k)2}(z)],\\
&\gamma_{31}^{(k)} = d_{31}^{(k)}(z)/S_{11}^{(k)}(z)[1 - \nu^{(k)2}(z)],\\
&k_p^{(k)2}(z) = 2d_{31}^{(k)2}(z)/\varepsilon_{33}^{T(k)}(z)[1 - \nu^{(k)}(z)], \quad \nu^{(k)} = -S_{12}^{(k)}/S_{11}^{(k)}(z);
\end{aligned} \tag{5}$$

$\sigma_{rr}^{(k)}$, $\sigma_{rr}^{(k)}$, $\sigma_{r\theta}^{(k)}$ are stresses, ε_r, ε_θ, $\varepsilon_{r\theta}$ are planar deformations, κ_r, κ_θ, $\kappa_{r\theta}$ are bending deformations, $D_z^{(k)}$denotes inductions, $E_z^{(k)}$ is the electric intensity; $S_{11}^{(k)}(z)$, $\varepsilon_{33}^{T(k)}(z)$ and $d_{31}^{(k)}(z)$ represent the complex compliance, permitivity

and piezoelectric characteristics of the piezo-active materials. Putting $\gamma_{31}^{(k)} = 0$ in (3), we obtain simplified constitutive equations for the passive orthotropic layer ($k = 0$). It is supposed that the electrodes between the passive and active layers are coated. On the electrodes the potential differences $V_1 = V_A$ ($k = 1$) and $V_2 = -V_A$ ($k = 2$) are given. On the inner electrodes the electric potential is zero. Let us put $S_{11}^{(1)} = S_{11}^{(2)}$, $S_{12}^{(1)} = S_{12}^{(2)}$, $d_{31}^{(1)} = -d_{31}^{(2)} = d_{31} \succ 0$, $h_1 = h_2$. Then $\gamma_{31}^{(1)} = -\gamma_{31}^{(2)} = \gamma_{31} \succ 0$. Integrating (4) over the thickness of the layers, we obtain the inductions $C^{(1)}, C^{(2)}$ in the top and bottom layers, respectively:

$$C^{(1)} = -\frac{V_A}{V_{10}} + \frac{V_{11}}{V_{10}}(\varepsilon_r + \varepsilon_\theta) + \frac{W_{11}}{V_{10}}(\kappa_r + \kappa_\theta), \quad C^{(2)} = -\frac{V_A}{V_{10}} + \frac{V_{21}}{V_{10}}(\varepsilon_r + \varepsilon_\theta) + \frac{W_{21}}{V_{10}}(\kappa_r + \kappa_\theta), \tag{6}$$

where

$$V_{10} = h_1/\gamma_{33}, \quad V_{11} = -V_{21} = h_1\gamma_{31}/\gamma_{33}, \quad W_{11} = W_{21} = \frac{1}{2}h_1(h_0 + h_1)\gamma_{31}/\gamma_{33}. \tag{7}$$

From (4) we obtain the electric intensity in the piezolayers:

$$E_Z^{(k)} = \frac{C^{(k)}}{\gamma_{33}^{(k)}(z)} - \frac{\gamma_{31}^{(k)}(z)}{\gamma_{33}^{(k)}(z)}[(\varepsilon_r + \varepsilon_\theta) + z(\kappa_r + \kappa_\theta)]. \tag{8}$$

Using the strain–displacement relations for bending deformations [9,10,17,19,20,27] $\kappa_1 = -\frac{\partial^2 w}{\partial r^2}$, $\kappa_2 = -\left(\frac{1}{r}\frac{\partial w}{\partial r} + \frac{1}{r^2}\frac{\partial^2 w}{\partial \theta^2}\right)$, $\kappa_{12} = -\frac{\partial}{\partial r}\left(\frac{1}{r}\frac{\partial w}{\partial \theta}\right)$, substituting (8) in (3) and integrating results throughout the thickness of the plate, we obtain the constitutive equations for the moments

$$M_{(r,\theta)} = -D_{11,21}\frac{\partial^2 w}{\partial r^2} - D_{12,22}\left(\frac{1}{r}\frac{\partial w}{\partial r} + \frac{1}{r^2}\frac{\partial^2 w}{\partial \theta^2}\right) + M_0, \; M_{r\theta} = -D_{66}\frac{\partial}{\partial r}\left(\frac{1}{r}\frac{\partial w}{\partial r}\right), \tag{9}$$

where w is the displacement in the z-direction,

$$\begin{aligned} D_{11,22} &= \frac{h_0^3}{12}B_{11,22}^{(0)} + \frac{2}{3}\left[\left(\frac{h_0}{2} + h_1\right)^3 - \left(\frac{h_0}{2}\right)^3\right]\left(B_{11,22}^{(1)} + \frac{\gamma_{31}^2}{\gamma_{33}}\right) - \frac{1}{2}\frac{\gamma_{31}^2}{\gamma_{33}}h_1\,(h_0 + h_1)^2\,, \\ D_{12} = D_{21} &= \frac{h_0^3}{12}B_{12}^{(0)} + \frac{2}{3}\left[\left(\frac{h_0}{2} + h_1\right)^3 - \left(\frac{h_0}{2}\right)^3\right]\left(B_{12}^{(1)} + \frac{\gamma_{31}^2}{\gamma_{33}}\right) - \frac{1}{2}\frac{\gamma_{31}^2}{\gamma_{33}}h_1\,(h_0 + h_1)^2\,, \end{aligned} \tag{10}$$

$$D_{66} = \frac{h_0^3}{12}B_{66}^{(0)} + \frac{2}{3}\left[\left(\frac{h_0}{2} + h_1\right)^3 - \left(\frac{h_0}{2}\right)^3\right]B_{66}^{(1)}; \quad M_0 = \gamma_{31}\,(h_0 + h_1)\,V_A. \tag{11}$$

Substituting (9) in the equation of motion

$$\frac{1}{r}\frac{\partial^2(rM_r)}{\partial r^2} - \frac{1}{r}\left(\frac{\partial}{\partial r} - \frac{1}{r}\frac{\partial^2}{\partial \theta^2}\right)M_\theta + \frac{2}{r^2}\frac{\partial^2(rM_{r\theta})}{\partial r\,\partial\theta} + p(r,\theta) + \tilde{\rho}\omega^2 w = 0,$$

we obtain a complex equation for the bending vibrations of a plate subject to mechanical and electrical loads:

$$\begin{aligned} &\frac{1}{r}\frac{\partial^2}{\partial r^2}\left(D_{11}r\frac{\partial^2 w}{\partial r^2}\right) + \left\{\frac{1}{r}\frac{\partial^2}{\partial r^2}\left[D_{12}\left(\frac{\partial w}{\partial r} + \frac{1}{r}\frac{\partial^2 w}{\partial r^2}\right)\right] + \frac{1}{r}\left(\frac{1}{r}\frac{\partial^2}{\partial \theta^2} - \frac{\partial}{\partial r}\right)\left(D_{12}\frac{\partial^2 w}{\partial r^2}\right)\right\} \\ &\quad + \frac{2}{r^2}\frac{\partial^2}{\partial r\,\partial\theta}\left[D_{66}r\frac{\partial}{\partial r}\left(\frac{1}{r}\frac{\partial w}{\partial \theta}\right)\right] + \frac{1}{r}\left(\frac{\partial^2}{\partial \theta^2} - \frac{\partial}{\partial r}\right)\left[D_{22}\left(\frac{1}{r}\frac{\partial w}{\partial r} + \frac{1}{r^2}\frac{\partial^2 w}{\partial \theta^2}\right)\right] - p\,(r,\theta) \\ &\quad - (\gamma h_0)\,\omega^2 w - \left[\frac{1}{r}\frac{\partial}{\partial r}\left(r\frac{\partial}{\partial r}\right) + \frac{1}{r^2}\frac{\partial^2}{\partial \theta^2}\right]M_0 = 0. \end{aligned} \tag{12}$$

Here γ is the density of the passive material,

$$w = w' + \mathrm{i}w'', \quad D_{ij} = D'_{ij} + \mathrm{i}D''_{ij}, \quad M_0 = M'_0 + \mathrm{i}M''_0, \quad i = \sqrt{-1}. \tag{13}$$

In cylindrical coordinates the energy equation for a thin orthotropic plate has the form [13]:

$$\frac{1}{r}\frac{\partial}{\partial r}\left(r\frac{\partial T}{\partial r}\right)+\frac{\lambda_2}{\lambda_1}\frac{1}{r^2}\frac{\partial^2 T}{\partial\theta^2}-\frac{2\alpha}{\lambda_1 h_0}(T-T_C)+\frac{W}{\lambda_1 h_0}=\frac{1}{a}\frac{\partial T}{\partial t}, \tag{14}$$

where $2\alpha=(\alpha^+ +\alpha^-)$, $T_C=(\alpha^+T^+ +\alpha^-T^-)/(2\alpha)$; α^+,α^- are the heat-transfer coefficients on the lower and upper surfaces of a plate with temperatures T^+, T^-; λ_j $(j=1,2)$ denotes the thermal conductivity; a is the temperature conductivity. In (14) the dissipative function W is defined as

$$W=\frac{\omega}{2}[(M_r''\kappa_r'-M_r'\kappa_r'')+(M_\theta''\kappa_\theta'-M_\theta'\kappa_\theta'')+2(M_{r\theta}''\kappa_{r\theta}'-M_{r\theta}'\kappa_{r\theta}'')+2(D_z''V_A'-D_z'V_A'')], \tag{15}$$

where $M_r=M_r'+\mathrm{i}M_r'',\ldots$.

The mechanical and the thermal boundary conditions have the standard form; see [21]. When only piezoelectric actuators are used, the main problem is to calculate the quantity M_0 for compensation of the mechanical load $p(r,\theta)$ and to investigate the influence of dissipative heating on M_0.

For open-circuit conditions the sensor voltage is given by

$$V_S=\frac{1}{\int_{(S)}\frac{\mathrm{d}S}{V_{10}}}\iint_{(S)}\frac{W_{11}}{V_{10}}(\kappa_r+\kappa_\theta)\mathrm{d}S, \tag{16}$$

where S is the area of sensor.

For short-circuit conditions the charge and the current of the sensors are given by

$$Q=2\iint_{(S)}\frac{W_{11}}{V_{10}}(\kappa_r+\kappa_\theta)\mathrm{d}S,\quad I=\dot{Q}. \tag{17}$$

To damp the forced vibrations of the plate, the actuator's potential difference is given:

$$V_A=-GI \text{ or } V_A=-G\dot{V}_S. \tag{18}$$

3 Solution of the problem by a variational method

The voltage V_A, applied to the actuator to compensate the mechanical load, and the sensor signal are integral parameters. The problem of ACD of plates can be solved effectively by variational methods. For example, consider the actively damped axisymmetric forced vibrations of a solid circular isotropic plate of radius R with built-in edge. Then the thermomechanical behavior of a plate subjected to a mechanical load $p_0(\rho)\exp(\mathrm{i}\omega t)$is described by a nonlinear system of differential equations in cylindrical coordinates:

$$\begin{aligned}
&\frac{1}{\rho}\frac{\mathrm{d}^2}{\mathrm{d}\rho^2}\left[D\left(\rho\frac{\mathrm{d}^2 w}{\mathrm{d}\rho^2}+\nu\frac{\mathrm{d}w}{\mathrm{d}\rho}\right)\right]+\frac{1}{\rho}\frac{\mathrm{d}}{\mathrm{d}\rho}\left[D\left(\nu\frac{\mathrm{d}^2 w}{\mathrm{d}\rho^2}+\frac{1}{\rho}\frac{\mathrm{d}w}{\mathrm{d}\rho}\right)\right]-(\gamma h_0)\ R^4\omega^2 w\ -\ R^4 p_0(\rho)\ =0,\\
&\frac{\mathrm{d}^2 T}{\mathrm{d}\rho^2}+\frac{1}{\rho}\frac{\mathrm{d}T}{\mathrm{d}\rho}-\frac{2\alpha R^2}{(\lambda h_0)}\left(T-T^0\right)+\frac{\omega E''(T)h_0^2}{24R^2\left(1-\nu^2\right)\lambda}\\
&\quad\times\left[\left(\frac{\mathrm{d}^2 w'}{\mathrm{d}\rho^2}\right)^2+\left(\frac{\mathrm{d}^2 w''}{\mathrm{d}\rho^2}\right)^2+\left(\frac{1}{\rho}\frac{\mathrm{d}w'}{\mathrm{d}\rho}\right)^2+\left(\frac{1}{\rho}\frac{\mathrm{d}w''}{\mathrm{d}\rho}\right)^2+2\nu\left(\frac{1}{\rho}\frac{\mathrm{d}w'}{\mathrm{d}\rho}\frac{\mathrm{d}^2 w'}{\mathrm{d}\rho^2}+\frac{1}{\rho}\frac{\mathrm{d}w''}{\mathrm{d}\rho}\frac{\mathrm{d}^2 w''}{\mathrm{d}\rho^2}\right)\right]=0.
\end{aligned} \tag{19}$$

Here $D=Eh_0^3/[12(1-\nu^2)]$, where E is the complex Young's modulus. The relationship between the viscoelastic parameters (μ,ν,E) is given by $E=2(1+\nu)\mu$, where μ, ν are the shear modulus and Poisson's ratio, respectively. In (19) $\rho=r/R$ is the non-dimensional radius. Hereafter we assume that ν is constant and μ is a linear function of the temperature:

$$\mu=G'+\mathrm{i}G'',\quad G'=G_0'-G_1'T,\quad G''=G_0''-G_1''T, \tag{20}$$

In (20) the constants G_0', G_0'', G_1', G_1'' are determined by experiment. For example, experimental date for a polyethylene are given in [28]. In the temperature range $20^\circ C\le\theta=T-T_C\le 80^\circ C$, we have

$$G'=968-8.69\theta(\mathrm{MPa}),\quad G''=87.1-0.7\theta(\mathrm{MPa}). \tag{21}$$

The Poisson ratio, density and thermal conductivity are $\nu = 0.3227$; $\gamma = 936\,\mathrm{kg/m}^3$; and $\lambda = 0.47\,\mathrm{W/(m\,K)}$, respectively. These data are used in the numerical calculations.

For a built-in edge and constant edge temperature the mechanical and thermal boundary conditions are

$$w = 0, \quad \frac{\mathrm{d}w}{\mathrm{d}\rho} = 0 \quad (\rho = 1), \tag{22}$$

$$\theta = T - T_C = 0 \quad (\rho = 1). \tag{23}$$

For open-circuit conditions the sensor voltage (16) in the cylindrical coordinate system are rewritten as

$$V_S = -\frac{h_1\,(h_0 + h_1)\int_0^{\rho_1} \frac{d_{31}}{S_{11}\,(1-\nu)}\nabla^2 w\rho \mathrm{d}\rho}{2R^2\int_0^{\rho_1}\varepsilon_{33}\left(1 - k_p^2\right)\rho \mathrm{d}\rho}; \quad \nabla^2 = \frac{\mathrm{d}^2}{\mathrm{d}\rho^2} + \frac{1}{\rho}\frac{\mathrm{d}}{\mathrm{d}\rho}, \tag{24}$$

where ρ_1 is the non-dimensional radius of the sensor.

If the sensor parameters do not depend on temperature, the expression (24) is represented as

$$V_S = -\frac{h_1\,(h_0 + h_1)}{2\rho_1^2 R^2}\,\frac{k_p^2}{d_{31}\left(1 - k_p^2\right)}\int_0^{\rho_1}\nabla^2 w\,\rho\,\mathrm{d}\rho. \tag{25}$$

The expression (25) does not change if the material characteristics depend on an area-averaged temperature. We assume in the following discussion that the Poisson ratio ν is a real value which does not depend on temperature. Therefore, to investigate the influence of the temperature on the sensor signal, it is necessary to solve the nonlinear system of differential equations (20)–(23) and substitute the obtained temperature due to dissipative heating in expression (24) or (25).

For the first mode of vibrations the approximation of the deflection is given by the expression

$$w = A\,\left(1 - \rho^2\right)^2. \tag{26}$$

Using (21), we obtain that the temperature of dissipative heating is determined by the equation

$$\frac{\mathrm{d}^2 T}{\mathrm{d}\rho^2} + \frac{1}{\rho}\frac{\mathrm{d}T}{\mathrm{d}\rho} - \frac{2\alpha R^2}{(\lambda h_0)}\,(T - T_C) + \frac{4\omega h_0^2 x}{3\,(1-\nu)\;R^2\lambda}\left(G_0'' - G_1'' T\right) f\,(p) = 0. \tag{27}$$

Here

$$x = |A|^2; \quad f\,(p) = (2 + 2\nu) - (8 + 8\nu)\,\rho^2 + (10 + 6\nu)\,\rho^4. \tag{28}$$

The thermal boundary conditions have the form (23).

The solution of the problem (23), (27) is reduced to minimization of the functional

$$F = \frac{1}{2}\int_0^1 \left[\left(\frac{\mathrm{d}\theta}{\mathrm{d}\rho}\right)^2 + \Psi_2(\rho)\theta^2 - 2\Psi_3(\rho)\theta\right]\,\rho\;\mathrm{d}\rho, \tag{29}$$

where

$$\begin{gathered}\Psi_2(\rho) = \Psi_4 + \Psi_1 f(\rho), \quad \Psi_3(\rho) = \Psi_0 f(\rho), \quad \Psi_4 = \frac{2\alpha R^2}{(\lambda h_0)}, \\ \Psi_1 = \frac{4\omega h_0^2 G_1''}{3\,(1-\nu)\,R^2\lambda}\,|A|^2, \quad \Psi_0 = \frac{4\omega h_0^2}{3\,(1-\nu)\,R^2\lambda}\tilde{G}_0'', \quad \tilde{G}_0'' = G_0'' - G_1'' T_C.\end{gathered} \tag{30}$$

The temperature is given by:

$$\theta = T_1\left(1 - \rho^2\right). \tag{31}$$

From (29) the parameter T_1 is determined by

$$T_1 = \frac{C_1 x}{C_0 + C_2 x}, \tag{32}$$

where

$$C_0 = 1 + \frac{1}{6}\psi_4, \quad C_1 = \left(1 + \frac{\nu}{12}\right)\psi_0, \quad C_2 = \left(\frac{1}{6} + \frac{\nu}{10}\right)\psi_1, \tag{33}$$

$$\psi_0 = \frac{8\omega}{\lambda h_0 R^2} D_0'', \quad \psi_1 = \frac{8\omega}{\lambda h_0 R^2} D_1'', \quad \psi_4 = \frac{2\alpha R^2}{\lambda h_0}. \tag{34}$$

The mechanical problem is reduced to a variational problem for the complex functional:

$$\ni = \frac{1}{2}\int_0^1 \left\{ \left(D' + \mathrm{i}D''\right) \left[\left(\frac{\mathrm{d}^2 w}{\mathrm{d}\rho^2}\right)^2 + \left(\frac{1}{\rho}\frac{\mathrm{d}w}{\mathrm{d}\rho}\right)^2 + \frac{2\nu}{\rho}\frac{\mathrm{d}w}{\mathrm{d}\rho}\frac{\mathrm{d}^2 w}{\mathrm{d}\rho^2} \right] - (\gamma h_0)\, R^4\omega^2 w^2 - 2p_0(\rho)R^4\omega \right\} \rho \mathrm{d}\rho. \tag{35}$$

The variational procedures for formulating forced vibrations of viscoelastic plates are appreciably more involved than in the corresponding classical problem for an elastic plate. In the classical problem it is assumed that the bending stiffness is real. In (35) it is complex: $(D' + \mathrm{i}D'')$.

Using the approximations (21), (26) and (31), by a standard variational procedure we get the complex amplitude of the plate vibrations:

$$A = \frac{p_0}{A_1 + \mathrm{i}A_2}, \tag{36}$$

where

$$A_1 = B_1 - b_1 T_1, \quad A_2 = B_2 - b_2 T_1, \quad B_1 = \frac{64 D_0'}{R^4} - \frac{3}{5}(\gamma h_0)\,\omega^2, \quad B_2 = \frac{64 D_0''}{R^4},$$
$$b_1 = \frac{96 D_1'}{R^4}\left(\frac{1}{4} + \frac{\nu}{12}\right), \quad b_2 = \frac{96 D_1''}{R^4}\left(\frac{1}{4} + \frac{\nu}{12}\right). \tag{37}$$

From (32) and (36) we may derive a cubic equation for the non-dimensional temperature $y = T_1/T_C$:

$$y^3 - e_2\, y^2 + e_1\, y - e_0 = 0, \tag{38}$$

where

$$e_0 = \frac{d_0}{T_C^3}, \quad e_1 = \frac{d_1}{T_C^2}, \quad e_2 = \frac{d_2}{T_C},$$
$$d_0 = \frac{C_1 q_0/C_0}{b_1^2 + b_2^2}, \quad d_1 = \frac{B_1^2 + B_2^2 + C_2 q_0^2/C_0}{b_1^2 + b_2^2}, \quad d_2 = 2\ \frac{b_1\ B_1 + b_2\ B_2}{b_1^2 + b_2^2}. \tag{39}$$

After determining the temperature, we find the amplitude $Z = \sqrt{x}$ for the vibrations of the plate, where

$$x = \frac{p_0^2}{\left(B_1^2 + B_2^2\right) - 2\ (b_1\ B_1 + b_2\ B_2)\ \ T_1 + \left(b_1^2 + b_2^2\right)\ T_1^2}. \tag{40}$$

Let us introduce the temperature averaged over the area of the sensor:

$$\bar{\theta} = T_1\left(1 - \frac{\rho_1^2}{2}\right). \tag{41}$$

Then we obtain the following expression for V_S:

$$V_S = 2h_1\ (h_0 + h_1)\, A \frac{k_p^2\left(\bar{T}\right)}{R^2 d_{31}\left(\bar{T}\right)\ \left[1 - k_p^2\left(\bar{T}\right)\right]}\left(1 - \rho_1^2\right). \tag{42}$$

Here k_p^2 is a planar coefficient for the electromechanical coupling [9,21].

The solution of the boundary-value problem (20)–(23) for a plate subjected to mechanical and electrical loads is reduced to solving a variational problem for the complex functional

$$\ni = \frac{1}{2}\int_0^1 \left\{ \left(D' + \mathrm{i}D''\right) \left[\left(\frac{\mathrm{d}^2 w}{\mathrm{d}\rho^2}\right)^2 + \left(\frac{1}{\rho}\frac{\mathrm{d}w}{\mathrm{d}\rho}\right)^2 + \frac{2\nu}{\rho}\frac{\mathrm{d}w}{\mathrm{d}\rho}\frac{\mathrm{d}^2 w}{\mathrm{d}\rho^2} \right] \right.$$
$$\left. - (\gamma\, h_0)\ R^4\omega^2 w^2 - 2p_0(\rho)R^4 w - 2M_0 R^2 \nabla^2 w \right\} \rho \mathrm{d}\rho. \tag{43}$$

It is seen from (43) that the potential difference of the actuator, which compensates the mechanical load, is given by

$$V_A = -\frac{R^2 \int_0^1 p_0(\rho) w \rho \mathrm{d}\rho}{\frac{1}{2}(h_0 + h_1) \int_0^{\rho_1} \gamma_{31}(\rho) \nabla^2 w \rho \mathrm{d}\rho}. \tag{44}$$

If the characteristics of the piezoactive material are independent of the temperature, we have from (44):

$$V_A = -R^2 \int_0^1 p_0 w \rho \mathrm{d}\rho \Big/ \left[\frac{1}{2}(h_0 + h_1)\gamma_{31} \int_0^{\rho_1} \nabla^2 w \rho \mathrm{d}\rho \right]. \tag{45}$$

For the temperature averaged over the area of the actuator we obtain

$$V_A = R^2 p_0 / [12(h_0 + h_1)\rho_1^2 \left(1 - \rho_1^2\right) \ \gamma_{31} \left(\bar{\theta}\right)]. \tag{46}$$

We consider the piezoactive material TsTS BS–2. The temperature dependence of the electromechanical parameters of the material given in [10]. Equation (44) shows that on resonance the temperature of dissipative heating does not influence the potential difference of the actuator to compensate the mechanical load if the mechanical characteristics of the passive material depend on temperature, but the electromechanical characteristics of the active materials do not. This is an important result. It gives the possibility to use the simple formula (45) to calculate the potential difference to compensate the mechanical load on resonance.

Using the second method of actively damped forced resonant vibrations, we calculate the quantity M_0 in the functional (43) as follows:

$$M_0 = -\mathrm{i}\omega m_0 F A, \tag{47}$$

where

$$m_0 = G\gamma_{31}^2 (h_0 + h_1)^2, \quad F = \iint_{(S_1)} \nabla^2 \tilde{w}(\rho) \rho \, \mathrm{d}\rho = 8\pi\rho_1^2(1 - \rho_1^2). \tag{48}$$

The amplitude of forced vibrations is calculated by (40), in which additional damping is obtained by replacement of the quantity B_2 by

$$\tilde{B}_2 = B_2 + G_2, \tag{49}$$

where

$$G_2 = \frac{24}{R^2} G\gamma_{31}^2 (h_0 + h_1)^2 \rho_1^2 (1 - \rho_1^2) F. \tag{50}$$

Figure 1 shows the dependence of the relative potential actuator's difference $K_A = |V_A(20°C| \,/\, |V_A(\theta°C|$ to compensate mechanical load on the amplitude of the load for temperature-dependent (solid line) and temperature-independent (dashed line) characteristics of the active material.

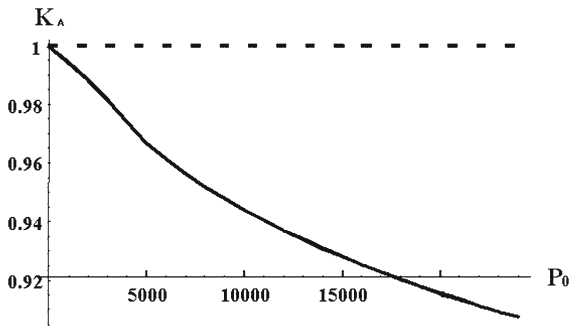

Fig. 1 Dependence of potential actuator difference on the amplitude of the load

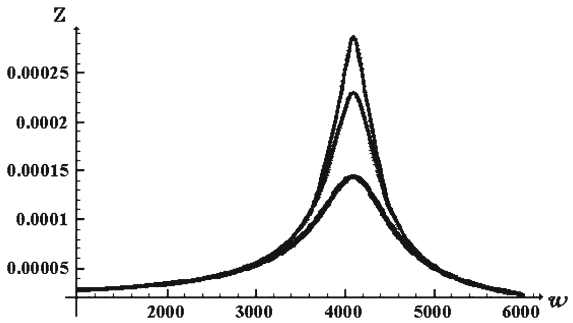

Fig. 2 Influence of the feedback-control gain G on the amplitude–frequency characteristics without taking into account the temperature dependence of the material properties

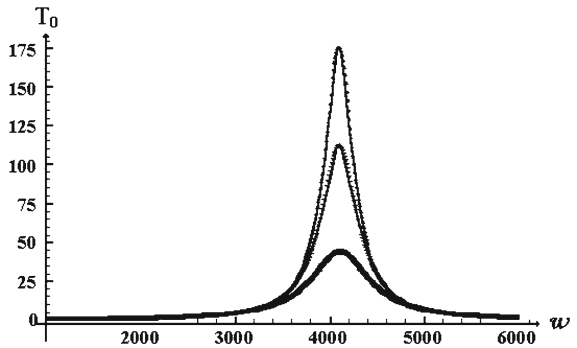

Fig. 3 Influence of the feedback-control gain G on the temperature–frequency characteristics without taking into account the temperature dependence of the material properties

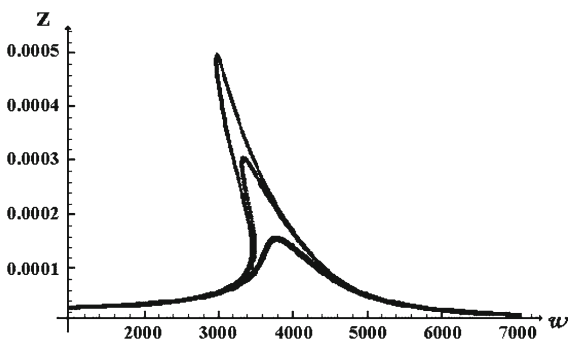

Fig. 4 Influence of the feedback-control gain G and the temperature resulting from dissipative heating on the amplitude–frequency characteristics

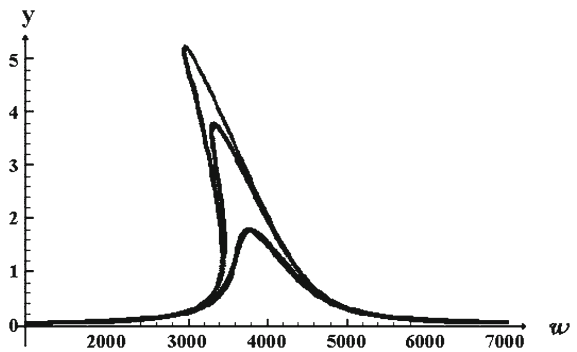

Fig. 5 Influence of the feedback-control gain G and the temperature resulting from dissipative heating on the temperature–frequency characteristics

The radius of the plate is $R = 0.0536\,\text{m}$ and its thickness is $h_0 = 0.01\,\text{m}$. Heat-transfer coefficients are $\alpha_1 = \alpha_2 = \alpha_S = \alpha = 0.5\text{W/(m}^2\,\text{K)}$. As is seen, the temperature resulting from dissipative heating reduces the efficiency of active-damping resonance vibrations of a circular plate.

Figures 2 and 3 illustrate the influence of the feedback-control gain G on the amplitude– and temperature–frequency characteristics under combined use of the actuators and sensors without taking into account temperature dependence of the material properties. The radius of the plate is $R = 0.1072\,\text{m}$. Heat-transfer coefficients are given as $\alpha_1 = \alpha_2 = \alpha_S = \alpha = 0.5\,\text{W/(m}^2\,\text{K)}$. The bottom, middle and upper curves correspond to $G = 0$, $\omega G = 0.5B_2$, $\omega G = 1.5B_2$, respectively.

The curves in Figs. 4 and 5 illustrate the influence of the temperature dependence of the material properties and the parameter G on the amplitude– and temperature–frequency characteristics under combined use of the actuators and sensors.

As is seen, the temperature dependence leads to a quality change of the amplitude– and temperature–frequency characteristics. They are typical for nonlinear systems. At the same time, an increase of feedback-control gain G reduces the amplitude of the vibrations. The influence of the physical nonlinearity eliminates the non-uniqueness of the amplitude– and temperature–frequency characteristics and reduces the temperature of dissipative heating.

4 Numerical solution of the problem of active vibration damping of a circular plate

Consider the problem of active vibration damping of a circular plate of inner and outer radiuses $r = r_0$ and $r = R$, respectively. The three-layer plate is composed of a passive inner layer and two piezoelectric outer layers of opposite

thickness polarization. On the outer surfaces of the piezolayers and on the surfaces between the active and passive layers the thin electrodes are placed. The plate is subjected to an axisymmetric harmonic pressure $q = p(r)\cos\omega t$ with frequency ω close to resonance. The electric potential difference is $\varphi(\frac{h_0}{2}+h_1)-\varphi(-\frac{h_0}{2}-h_1) = 2\Re\mathfrak{e}(V_A e^{\mathrm{i}\omega t})$, where $V_A = V_A' + \mathrm{i}V_A''$. On the inner electrodes the electric potential is zero. The materials of the layers are viscoelastic. On the surfaces of the plate a heat transfer by convection occurs. Simply supported and built-in edges of the plate are considered. The coupled problem of forced plate vibrations is described by a complex system of differential equations (12), which can be written in normal form

$$\begin{gathered}\frac{\mathrm{d}w}{\mathrm{d}r} = -\vartheta, \quad \frac{\mathrm{d}\vartheta}{\mathrm{d}r} = \frac{\nu_D}{r}\vartheta + J_D M_r - J_D M_E, \\ \frac{\mathrm{d}M_r}{\mathrm{d}r} = D_{11}(1-\nu_D^2)\frac{\theta}{r^2} - \frac{1+\nu_D}{r}M_r + Q_r - \frac{1+\nu_D}{r}M_E, \quad \frac{\mathrm{d}Q_r}{\mathrm{d}r} = -\gamma\bar{h}\omega^2 w - Q_r - p\,(r)\end{gathered} \tag{51}$$

with boundary conditions

$$w = M_r = 0 \ \ (r = r_0;\ R) \quad \text{or } w = \vartheta = 0 \ \ (r = r_0;\ \ R). \tag{52}$$

The energy equation (14) is

$$\frac{1}{a}\frac{\partial T}{\partial t} = \frac{\partial^2 T}{\partial r^2} + \frac{1}{r}\frac{\partial T}{\partial r} - \frac{2\alpha_s}{\lambda H}(T - T_c) + \frac{1}{\lambda H}\bar{W}, \tag{53}$$

where the nonlinear dissipative function is given by

$$\begin{aligned}\bar{W} = \frac{\omega}{2}\Big[D_{11}''\left(\kappa_r'^2 + \kappa_r''^2 + \kappa_\theta'^2 + \kappa_\theta''^2\right) + 2D_{12}''\left(\kappa_r'\kappa_\theta' + \kappa_r''\kappa_\theta''\right) + 2\left(h_0+h_1\right)b_{31}''\left(\kappa''V' + \kappa'V''\right) \\ + 2b_{33}''\left(V'^2 + V''^2\right)/h_1\Big].\end{aligned} \tag{54}$$

The thermal boundary and initial conditions are

$$\frac{\partial T}{\partial r} = \pm\frac{\alpha_{1,2}}{\lambda}(T - T_c) \quad (r = r_0,\ R), \quad T = T_0 \ \ (t = 0). \tag{55}$$

The electric intensity E_z and induction D_z become

$$\begin{gathered}E_z = -\frac{V_A}{h_1} + \frac{b_{31}}{b_{33}}\left(\frac{h_0+h_1}{2} \pm z\right)\kappa, \quad \left(-\frac{h_0}{2} - h_1 \le z \le -\frac{h_0}{2};\ \ \frac{h_0}{2} \le z \le \frac{h_0}{2} + h_1\right), \\ D_z = -b_{33}\frac{V_A}{h_1} + b_{33}\frac{h_0+h_1}{2}\kappa,\end{gathered} \tag{56}$$

where

$$\begin{gathered}D_{1m} = \frac{h_0^3}{12}c_{1m} + \frac{1}{6}\left(4h_1^3 + 6h_1^2h_0 + 3h_1h_0^2\right)c_{1m}^E + \frac{1}{6}\gamma_{31}h_1^3, \quad (m = 1, 2), \\ c_{11} = \frac{E}{1-\nu^2}, \quad c_{11}^E = \frac{1}{s_{11}^E\left(1-\nu_E^2\right)}, \quad \gamma_{31} = \frac{b_{31}^2}{b_{33}}, \quad c_{12} = \nu c_{11}, \quad c_{12}^E = \nu_E c_{12}^E, \\ \nu_E = -\frac{s_{12}^E}{s_{11}^E}, \quad b_{31} = \frac{d_{31}}{s_{11}^E\left(1-\nu_E\right)}, \quad b_{33} = \varepsilon_{33}^T\left(1 - k_p^2\right), \\ M_E = b_{31}\left(h_0+h_1\right)V_A, \quad \kappa = \kappa_r + \kappa_\theta, \quad \kappa_r = \frac{\mathrm{d}\vartheta}{\mathrm{d}r}, \quad \kappa_\theta = \frac{\vartheta}{r}, \quad J_D = 1/D_{11}, \\ E\,(T) = E' + \mathrm{i}E'', \quad \gamma\bar{h} = \gamma h_0 + 2\gamma_* h_1, \quad H = h_0 + 2h_1, \quad \nu_D = -D_{12}J_D, \\ s_{11}^E\,(T) = s_{11}'\left(1 - \mathrm{i}\delta_{11}\right), \quad d_{31}\,(T) = d_{31}'\left(1 - \mathrm{i}\delta_{31}\right), \quad \varepsilon_{33}^T = \varepsilon_{33}'\left(1 - \mathrm{i}\delta_{33}\right).\end{gathered} \tag{57}$$

Here γ, γ_* are the densities of the passive and piezo-active materials; α_s is the heat-transfer coefficient on the surfaces $r = r_0$, $r = R$; $\alpha_{1,2}$ are the heat-transfer coefficients on the lower surface $z = h_0/2$ and upper surface $z = -h_0/2$; λ, a are the thermal conductivity and temperature conductivity. If the characteristics of the materials are independent of the temperature, the coupled problem is reduced to the solution of a linear mechanical problem, the calculation of

the dissipative function and the solution of a linear heat- conduction equation with internal heat generation W.The nonlinear coupled problem (51)–(55) is solved by a step-by-step integration in time [10,12,13]. To integrate the system of differential equations, a discrete orthogonalization method is used [27]. For $p(r) = p_0 = \text{const}$ relation (44) can be written as

$$V_A = k_A p_0, \tag{58}$$

where

$$k_A = -\frac{R^2 \int_{r_0}^{R} wr\,\mathrm{d}r}{(h_0 + h_1) \int_{r_1}^{r_2} b_{31} (\kappa_r + \kappa_\theta)\, r\,\mathrm{d}r}. \tag{59}$$

Another way of looking at it is to find amplitudes $w_{P\max}$ and $w_{E\max}$ at resonance for $p_0 = 1\text{Pa}$, $V_A' = V_A'' = 0$ and $p_o = 0$, $V_A' = 1\text{V}$, $V_A'' = 0$, respectively. Then

$$k_A = -\frac{w_{P\max}}{w_{E\max}}. \tag{60}$$

Three types of piazo-actuators are considered, namely for the piezo-active areas (i) $r_0 \le r \le r_1$; (ii) $r_2 \le r \le R$; (iii) $r_1 \le r \le r_2$. Introduce the non-dimensional quantities $x(r) = (r - r_0)/L$, $L = R - r_0$; $\tau = at/L^2$; $\gamma_S = \alpha_S L/\lambda$; $\gamma_{1,2} = \alpha_{1,2} L/\lambda$. Numerical results are obtained for a plate composed of the above-mentioned passive and piezo-active materials. The geometric sizes and heat-transfer parameters are chosen as $r_0 = 0.05\,\text{m}$, $R = 0.2\,\text{m}$, $h_0 = 0.01\,\text{m}$, $\gamma_1 = 0$, $\gamma_2 = \gamma_S = 0.638$.

For material properties independent of the temperature, the numerical results for the calculations of vibration characteristics are shown in Figs. 6a, 7a for simply supported edges and in Figs. 6b, 7b for built-in edges. The curves $1, 1'; 2, 2'; 3, 3'$ were calculated for the cases (i) $(0 \le x \le x_1, \Delta_1 = x_1)$; (ii) $x_2 \le x \le 1, \Delta_2 = x_2)$; (iii) $x_1 \le x \le x_2, \Delta_3 = x_2 - x_1, x_i = x(r_i)$, respectively. The curves $1, 2, 3$ and $1', 2', 3'$ correspond to $h_1 = 0\,\text{m}$ and $h_1 = 0.5 \times 10^{-4}\,\text{m}$, respectively. For case (iii) a quantity Δ_3 is so chosen that the width of the actuator is symmetrical about a point $x_3 = 0.5$, where the amplitude of the vibrations is maximum. If $h_1 \neq 0$, the natural

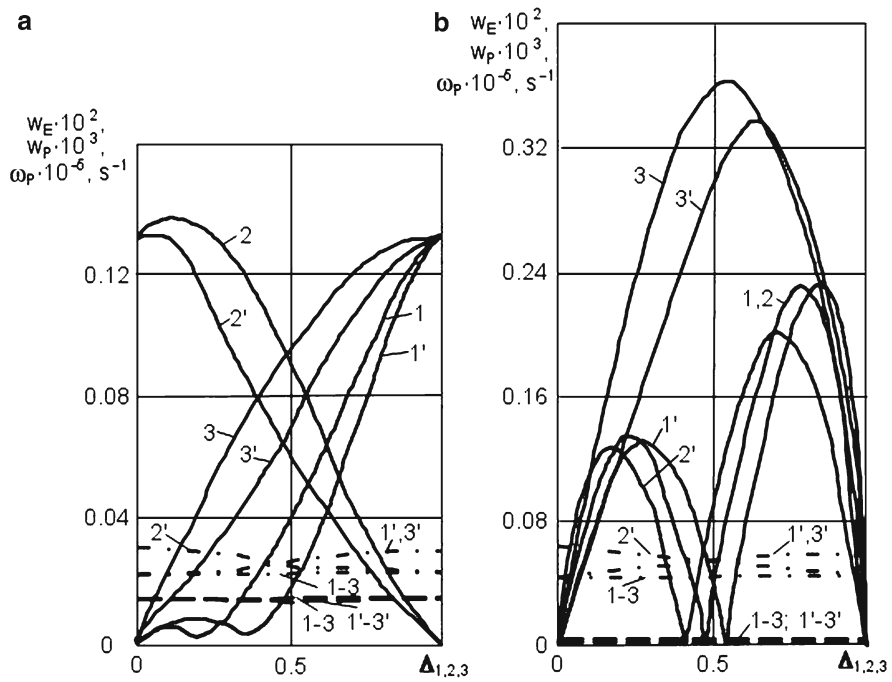

Fig. 6 Dependence of the characteristics of the actuator on its geometrical parameters

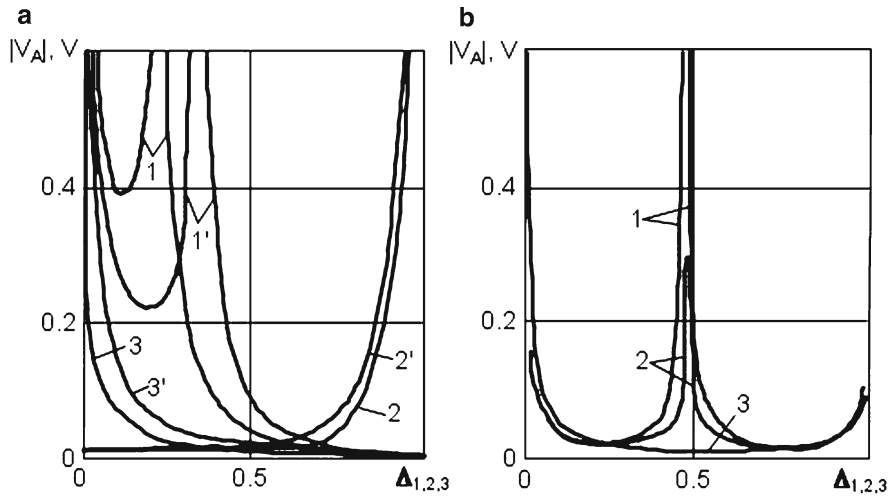

Fig. 7 Dependence of the amplitude of the electric potential difference on the width of the actuator

frequency ω_p increases with the size of the actuator (dash-primed curves) and is maximum for total coat. For small actuator thickness the size of the actuator only weakly influences the displacement amplitude $w_p = |w|/(2h_0)$ under the mechanical loading $p_0 = 1$ Pa; $V_A' = V_A'' = 0$ (dashed curves). For simply supported edges the amplitude $w_E = |w|/(2h_0)$ depends strongly on thickness, width and location of the actuator under the electric load $p_0 =$ 0Pa; $V_A' = 1$V, $V_A'' = 0$V (solid curves 1–3, 1′–3′ in Fig. 6a). For case (i) (curves 1, 1′) the amplitude of the displacement is an unambiguous function of Δ_1 for $\Delta_1 \prec 0.4$, then it abruptly increases and attains a maximum for total coat. For case (ii) (curves 2, 2′) the amplitude of the displacement increases monotonically with Δ_2 and attains a maximum for $\Delta_2 \approx 0.1$ (curve 2). But the effect decreases for increasing actuator thickness (curve 2′). For case (iii) (curves 3, 3′) the amplitude of the displacement increases with Δ_3. It is a single-valued function that has a maximum for total coat.

For built-in edges the curves differ qualitatively from those for simply supported edges. They are nonlinear and ambiguous. For cases (i) and (ii) the curves 1,2 reach a maximum for some width of the actuator ($\Delta_1 = \Delta_2 =$ 0.24; 0.76) and a minimum for ($\Delta_1 = \Delta_2 = 0$; 0.46; 1.0). For case (iii) (curve 3) the amplitude reaches a maximum for $\Delta_3 = 0.55$ ($x_1 = 0.225$; $x_2 = 0.775$). An increase of the actuator thickness (curves 1′–3′) will affect the width of the actuator for which the amplitudes are maximum or minimum.

Figure 7 shows the dependence of the amplitude of the electric potential difference on the width of the actuator as a result of a compensation of a unit mechanical load. Here we use the previous notations. For built-in edges the coefficients $k_{A\cdot 1}, k_{A2}$ are calculated by Eqs. (59), (60), respectively. For case (iii) these coefficients are shown in Table 1 for distinct parameters Δ_3 and h_1.

For simply supported edges, the actuator with total coat is most effective. If the width of the actuator decreases ($\Delta_i \leq 0.5L$), the coefficient of the control greatly increases.

Figure 8 shows amplitude–frequency (curve 1–4, $w^\bullet = 10 \cdot w(0.5)/h$) and temperature–frequency characteristics (curves $1^\bullet - 4^\bullet$, $T_{\max} - T(0)$) for simply supported plate edges. The plates are loaded by $p_0 = 0.8 \times 10^3$ Pa. The solid lines and dashed lines correspond to the cases when the material properties are temperature dependent and when they are independent of temperature, respectively. Curves 1–4 correspond to the following plate parameters: (i) $h_1 = 0$, $x_1 = 0$, $x_2 = 1$; (ii) $h_1 = 0.5 \times 10^{-4}$ m, $x_1 = 0$, $x_2 = 1$; (iii) $h = 0$, $x_1 = 0.25$, $x_2 = 0.75$; (iv) $h_1 = 0.5 \times 10^{-4}$ m, $x_1 = 0.25$, $x_2 = 0.75$.

For temperature-independent properties we have (a) $|V_A| = 9.4$ V; (b) $|V_A| = 9.37$ V; (c) $|V_A| = 12.95$ V;(d) $|V_A| = 15.6$ V.

For temperature-dependent properties we obtain (a) $|V_A| = 9.26$ V; (b) $|V_A| = 9.14$ V; (c) $|V_A| = 12.44$ V; (d) $|V_A| = 15.6$ V.

Table 1 Numerical values of potential difference, calculated by formulas by (59), (60) respectively

	$h_1 = 0\,\mathrm{m}$		$h_1 = 0.5 \times 10^{-4}\,\mathrm{m}$	
Δ_3	$\lvert k_{A1}\rvert \cdot 10$	$\lvert k_{A2}\rvert \cdot 10$	$\lvert k_{A1}\rvert \cdot 10$	$\lvert k_{A2}\rvert \cdot 10$
0.10	0.348	0.346	0.606	0.625
0.20	0.200	0.180	0.318	0.286
0.30	0.130	0.128	0.178	0.179
0.40	0.107	0.106	0.132	0.131
0.50	0.098	0.097	0.109	0.109
0.54	0.096	0.096	0.104	0.104
0.56	0.097	0.096	0.103	0.102
0.60	0.098	0.097	0.099	0.100
0.70	0.108	0.108	0.102	0.102
0.80	0.139	0.137	0.118	0.116
0.90	0.202	0.241	0.155	0.169

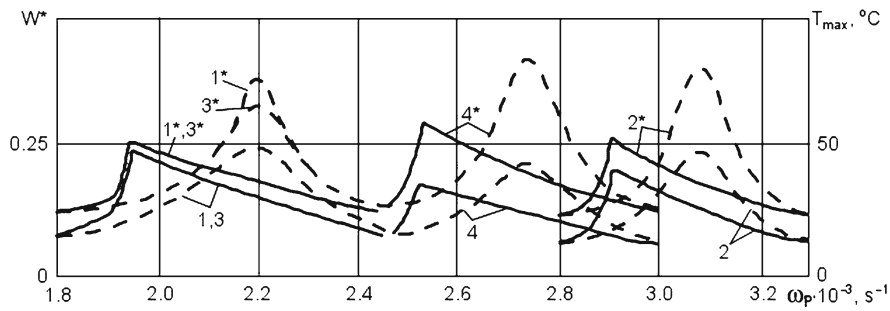

Fig. 8 Amplitude–frequency and temperature–frequency characteristics for simply-supported plate edges

As can be seen, the temperature dependence has only a weak influence on the effectiveness of damping by the actuators. A comparison of the curves 1 and 3 or 2 and 4 shows that the width has a weak effect on the maximum deflection and heating temperature for a given thickness of the actuator, but it changes the resonant frequency of system. Temperature dependency leads to a decrease of resonant frequency and to nonlinear amplitude– and temperature–frequency characteristics.

5 Conclusions

In this paper a mathematical formulation has been given for a new problem of actively damped vibrations of thin viscoelastic plates, with dissipative heating taken account as a result of a transformation of the electromechanical energy into thermal energy for resonant harmonic vibrations. Two methods of active damping are considered when (i) piezoelectric actuators are used and (ii) piezoelectric sensors and actuators are used. To investigate the influence of the temperature resulting from dissipative heating on the effectiveness of active vibration damping, it is necessary to solve a nonlinear boundary-value problem. To this end analytical and numerical methods have been used.

The problem of active axisymmetric damping vibrations of a circular plate with simply supported and built-in edges has been investigated. It is shown that for resonant vibrations the temperature of dissipative heating has no influence on the potential difference to compensate the mechanical load if the mechanical characteristics of the passive materials depend on temperature but the characteristics of the active materials do not. The result simplifies

the problem of calculating the aforementioned potential difference. The numerical results show that the effectiveness of the active damping vibrations of a circular plate decreases when taking into account the temperature dependence of the piezomaterial.

Under the combined use of a sensor and actuators for resonant vibration damping of circular plates, the temperature dependence of the characteristics leads to a qualitative change of the amplitude– and temperature–frequency characteristics which show a typical behavior for nonlinear systems. An increase of feedback-control gain reduces the influence of dissipative heating.

References

1. Birman V (1996) Thermal effects on measurements of dynamic processes in composite structures using piezoelectric sensors. Smart Mater Struct 5:379–385
2. Heidary F, Eslami NR (2005) Pyroelectric effect on dynamic response of coupled distributed piezothermoelastic composite plate. J Therm Stresses 28:285–300
3. Tzou HS, Howard RV (1994) A piezothermoelastic thin shell theory applied to active structures. J Vibration Acoust 116:295–302
4. Tzou HS, Ye R (1994) Piezothermoelasticity and precision control of piezoelectric systems: theory and finite element analysis. J Vibration Acoust 116:489–495
5. Tauchert TR, Ashida F (2003) Control of transient response in intelligent piezothermoelastic strustures. J Therm Stresses 26:559–582
6. Lu X, Hanagud SV (2004) Extended irreversible thermodynamics modeling for self-heating and dissipation in piezoelectric ceramics. IEEE Trans Ultrason Ferroelectr Freq Control 51:1582–1592
7. Mauk LD, Lynch CS (2003) Thermo-electro-mechanical behavior of ferroelectric materials. Part I: a computational micromechanical model versus experimental results. J Intell Mater Syst Struct 14:587–602
8. Mauk LD, Lynch CS (2003) Thermo-electro-mechanical behavior of ferroelectric materials. Part II: Introduction of rate and self-heating effects. J Intell Mater Syst Struct 14:605–620
9. Grinchenko VT, Ulitko AF, Shul'ga NA (1989) Electroelasticity. Naukova Dumka, Kiev, p 290
10. Karnaukhov VG, Kirichok IF (1989) Electrothermoviscoelasticity. Naukova Dumka, Kiev, p 320
11. Karnaukhov VG (1993) Modeling vibrations and dissipative heating of inelastic bodies. Prikl Mekh 29:70–76
12. Karnaukhov VG (1982) Coupled problems of thermoviscoelasticity. Naukova Dumka, Kiev, p 260
13. Karnaukhov VG, Kirichok IF (1986) Coupled problems of theory of viscoelastic plates and shells. Naukova Dumka, Kiev, p 220
14. Karnaukhov VG, Mikhailenko VV (2005) Nonlinear thermomechanics of piezoelectric nonelastic bodies under monoharmonic loading. ZTU, Zytomyr, p 428
15. Tzou HS, Bao Y (1997) Nonlinear piezothermoelasticity and multi-field actuations, part 1. Nonlinear anisotropic piezothermoelastic shell laminates. J Vibration Acoust 119:374–381
16. Tzou HS, Zhou YH (1997) Nonlinear piezothermoelasticity and multi-field actuations, part 2. Control of nonlinear deflection, buckling and dynamics. J Vibration Acoust 119:382–389
17. Gabbert U, Tzou HS (2001) Smart structures and structronic systems. Kluwer Academic Publication, Dordrecht, p 384
18. Tani J, Takagi T, Qiu J (1998) Intelligent material systems: applications of functional materials. Appl Mech Rev 51:505–521
19. Tzou HS, Bergman LA (1998) Dynamics and control of distributed systems. Cambridge University Press, Cambridge, p 400
20. Tzou HS (1993) Piezoelectric shells (Distributed sensing and control of continua). Kluwer Academic Publication, Dordrecht, p 400
21. Karnaukhov VG, Kirichok IF (2000) Forced harmonic vibrations and dissipative heating-up of viscoelastic thin-walled elements. Int Appl Mech 36:174–196
22. Karnaukhov VG, Kirichok IF, Kozlov VI (2001) Electromechanical vibrations and dissipative heating of viscoelastic thin-walled piezoelements. Int Appl Mech 37:182–212
23. Senchenkov IK, Zhuk Ya A, Karnaukhov VG (2004) Modelling the thermomechanical behavior of physically nonlinear materials under monoharmonic loading. Int Appl Mech 40:3–34
24. Karnaukhov VG, Mikhailenko VV (2002) Nonlinear single-frequency vibrations and dissipative heating of inelastic piezoelectric bodies. Int Appl Mech 38:521–547
25. Karnaukhov VG (2004) Thermal failure of polymeric structural elements under monoharmonic deformation. Int Appl Mech 40:3–30
26. Karnaukhov VG (2005) Thermomechanics of coupled fields in passive and piezoactive inelastic bodies under harmonic deformations. J Therm Stresses 28:783–815
27. Grigorenko Ya M, Vasilenko AT (1981) Theory of variable stiffness shells. Naukova Dumka, Kiev, p 544
28. Mason WP (ed) (1985) Physical acoustics, principles and methods. Properties of polymers and nonlinear acoustics, Vol II. Part B. Academic Press, New York, p 420